water

MDPI

Article

Tracing Groundwater Recharge Sources and Controls on Groundwater Quality in a Delineated Aquifer to Support Groundwater Allocation, De Aar, Northern Cape, South Africa

Lucky Baloyi [1,2,*], Sikelela Mqhayi [2], Harrison Pienaar [3,4], Mxolisi B. Mukhawana [5], Mike Butler [6] and Thokozani Kanyerere [2]

1 Department of Water and Sanitation, 52 Voortrekker Road, Belville Office, Cape Town 7530, South Africa
2 Department of Earth Science, University of the Western Cape, Bellville, Cape Town 7535, South Africa; smqhayi@uwc.ac.za (S.M.); tkanyerere@uwc.ac.za (T.K.)
3 Centre for Environmental Management, Faculty of Natural and Agricultural Science, University of the Free State, Bloemfontein 9300, South Africa; hhp4water@gmail.com
4 Institute of Africa Water Resources and Environmental Engineering, Handan 056000, China
5 Department of Water and Sanitation, 178 Francis Baard Street, Pretoria 0001, South Africa; mukhawanam@dws.gov.za
6 iThemba Labs, Environmental Isotope Laboratory, Private Bag 11, Wits, Johannesburg 2050, South Africa; mj.butler@ilabs.nrf.ac.za
* Correspondence: baloyil2@dws.gov.za; Tel.: +27-828759029

Abstract

Groundwater-dependent communities such as De Aar require a better understanding of groundwater systems to ensure sustainable allocation. This study aims to trace recharge sources in unconfined and confined aquifers and identify processes controlling groundwater quality using hydrogeochemistry and environmental tracers. It argues that aquifer delineation and hydraulic parameters alone cannot fully identify recharge sources or geochemical processes; integrating them with hydrogeochemistry and environmental tracers provides stronger evidence to support groundwater allocation. To validate the argument, the study integrated hydrogeochemical analysis, stable isotopes, tritium, radon-222, and statistical methods supported by depth-specific groundwater sampling. The results, interpreted using Piper and Gibbs diagrams, PHREEQC modelling, and scatter plots, show that groundwater evolution is mainly controlled by rock–water interaction, ion exchange, evaporation, and mixing processes. Ca–HCO_3 water indicates recent recharge, while Na–Cl water reflects evaporation effects in both unconfined and confined aquifers, with halite dissolution contributing to Na and Cl enrichment. Isotope results indicate that unconfined aquifer water is isotopically enriched and linked to recent recharge, whereas confined aquifer and spring waters are depleted, suggesting recharge from higher elevations through fractured zones. Tritium dating reveals young (<30 years), intermediate (30–50 years), and old groundwater (60–109 years), while radon results indicate active groundwater flow path, particularly along fractures. These findings demonstrate that groundwater recharge is derived from both local meteoric sources and regional contributions, resulting in predominantly fresh groundwater; however, localized quality concerns should be considered for improved water allocation.

Keywords: hydrogeochemistry; radon; recharge source; stable isotopes; tritium

Academic Editor: Chin H Wu

Received: 30 March 2026
Revised: 23 April 2026
Accepted: 25 April 2026
Published: 1 May 2026

1. Introduction

Groundwater is the primary and often the only reliable water resource in many semi-arid regions, including De Aar, Northern Cape, South Africa, where surface water availability is limited and highly variable. Increasing water demand for domestic, agricultural, and industrial activities has intensified pressure on groundwater resources, making groundwater allocation a critical challenge. Therefore, groundwater allocation should consider recharge as a key indicator of groundwater availability within a catchment, while also requiring a comprehensive understanding of recharge sources and the geochemical processes controlling groundwater quality. Although isotopes and hydrogeochemical methods have been widely used to investigate groundwater recharge, limited studies integrate these approaches within delineated fractured aquifer systems in semi-arid regions, leading to uncertainty in identifying recharge source and groundwater allocation. Building on the aquifer delineation study conducted by Baloyi et al. [1], this study proposes that identifying recharge sources and the processes controlling groundwater quality should be undertaken within a delineated aquifer system, integrating hydrogeochemistry, stable isotopes ($\delta^{18}O$ and $\delta^{2}H$), and environmental tracers such as tritium (^{3}H) and radon (^{222}Rn) in groundwater studies [2]. The influence of recharge water chemistry and subsurface geological processes on groundwater composition is consistent with the dominance of mineral weathering and carbonate dissolution observed in De Aar [3]. The hydrogeochemical differentiation between unconfined Ca–HCO_3-type and confined Na–Cl-type groundwater supports findings from Busan City, Korea, where similar facies were attributed to ion exchange, carbonate weathering, and evaporation, implying comparable groundwater evolution processes despite contrasting climatic settings [4]. Observations from fractured-rock aquifers in the Western Karoo, South Africa, further support the progression from fresh recharge waters to more evolved Na–Cl-type groundwater along regional flow paths, aligning with the isotopically depleted signatures and elevated radon (^{222}Rn) activities identified in the confined aquifer [5]. The dominance of dissolution, mixing, and ion exchange processes reported by Kumar et al. [6] in semi-arid and arid regions reinforces the conclusion that rock–water interaction is the primary control on groundwater quality. Collectively, these implications confirm that the aquifer systems are governed by natural geochemical evolution linked to meteoric recharge, residence time, and regional flow dynamics, providing a robust scientific basis for sustainable groundwater management in these groundwater-dependent communities. The reviewed studies provide a strong foundation for the current study's aim to develop a framework for tracing recharge sources, conducting hydrogeochemical characterization, and improving the understanding of groundwater quality in De Aar's aquifers.

Environmental tracers, particularly stable isotopes ($\delta^{2}H$ and $\delta^{18}O$), are widely used in groundwater studies to improve understanding of recharge sources, mixing processes, mineralization, and groundwater residence times [7,8]. Variations in $\delta^{2}H$ and $\delta^{18}O$ reflect isotopic fractionation during evaporation and condensation, allowing recharge sources to be traced through comparison with meteoric water signatures [9]. Waters plotting along the meteoric water line indicate direct atmospheric recharge, while deviations reflect evaporation or water–rock interaction [9]. Isotopic composition of precipitation is primarily controlled by temperature, latitude, altitude, and seasonality [10], while in semi-arid environments, recharge is often dominated by focused infiltration from surface water bodies rather than diffuse rainfall due to low precipitation and high evapotranspiration [11]. Although isotope hydrology has been applied globally and within South Africa, many studies in Southern Africa have emphasized aquifer yield, sustainability, or hydraulic connectivity rather than explicitly identifying recharge sources within delineated aquifer systems [12]. Enriched groundwater isotopic signatures typically indicate focused recharge

from surface water or geothermal sources, whereas depleted signatures suggest diffuse rainfall recharge [13]. Similar limitations have been noted in Western Africa, where isotopic studies commonly confirm meteoric recharge but rarely distinguish recharge pathways through the unsaturated zone, demonstrating the importance of defining both global and local meteoric water lines [14,15]. Addressing this gap, the present study applies stable isotope analysis to the delineated aquifer system to identify recharge source, thereby directly supporting the study's objective to use isotopic analysis to trace groundwater recharge sources using the De Aar aquifer as an example.

In line with the aim of this study, which is to trace groundwater recharge sources and identify the processes influencing groundwater quality within the delineated aquifer system, radioactive isotopes, especially tritium (^{3}H) and radon (^{222}Rn), are employed as key environmental isotopic tracers [13]. Studies worldwide indicate that radon-222 levels are typically higher in igneous rocks and shallow fractured aquifers, moderate in sedimentary rocks, and low in high-grade metamorphic rocks, making it a sensitive indicator of recharge sources and aquifer connectivity. Similarly, tritium (^{3}H) has also been widely applied in groundwater studies to investigate recharge processes, groundwater residence time, and flow dynamics, particularly in shallow unconfined aquifers and intermediate semi-confined aquifer systems [16,17]. As a naturally occurring cosmogenic isotope with a half-life of 12.32 years, tritium enters the hydrological cycle through precipitation and becomes incorporated into recharging groundwater [17]. Consequently, its concentration in groundwater reflects both the timing and magnitude of recharge, making it especially effective for distinguishing recently recharged (young) groundwater from older, regionally recharged groundwater [13]. Numerous studies have shown that elevated tritium levels are indicative of post-1950s recharge associated with atmospheric nuclear weapons testing, whereas low or non-detectable tritium concentrations generally signify longer residence times and deeper or regionally recharged groundwater systems [16,18]. In the semi-arid and fractured-rock setting characteristic of the De Aar area, the application of tritium directly supports the study objectives by enabling the identification of recharge sources, evaluating hydraulic connectivity between unconfined and confined aquifers, and constraining groundwater flow paths. When integrated with hydrogeochemical data and complementary isotopic tracers, tritium analysis provides a robust framework for interpreting recharge mechanisms, mixing processes, and the implications of groundwater age on water quality and sustainable groundwater use [19].

2. Description of the Study Area

2.1. Locality Setting

The study was conducted in De Aar, a town in the Northern Cape Province of South Africa, within the Vaal–Orange Catchment Management Agency (VOCMA). It lies in the Lower Orange Water Management Area (WMA), covering a portion of the quaternary catchment regions D62C and D62D (Figure 1a). The study area covers approximately 2226 km^2 and is located in the Eastern Karoo physiographic area at an elevation of 1100–1600 m.a.s.l. and forms part of the Brak River catchment. Following Baloyi et al. [1] catchment delineations, the study area was divided into three sub-catchments: the lower catchment, 1183–1233 m.a.s.l., the middle catchment, 1233–1261 m.a.s.l., and the upper catchment, 1261–above 1600 m.a.s.l. Figure 1b shows the location of the study area in De Aar, Northern Cape, South Africa. The registered volume of groundwater abstraction by the Municipality is approximately 9,560,356 Mm^3/annum (estimated from DWS WARMS registered volumes), which is about 34% of the average annual rainfall (250–300 mm) derived from the groundwater reserve report [20]. The rainfall occurs during the summer months, particularly between November and April each year. The average monthly temperature ranges

from about 23 °C in January to 8 °C in July. In the transitional months of March and April, daily temperatures typically vary between 15 °C and 17 °C. Winter months are often cold, with temperatures dropping to between 3 °C and –10 °C, while summers are hot, reaching up to 40 °C. Geomorphologically, the study area features scattered rings of dolerite hills covering approximately 50–60 km^2, with diameters of up to 12 km. These hills consist of horizontally layered dolerite sheets [21]. Overall, the region is classified as lowland, interspersed. The Brak River primarily drains the catchment that originates southeast of Hanover and several smaller tributaries (Figure 1a). These rivers generally exhibit short annual flow cycles, typically triggered by intense rainfall events. The intermediate valley regions are frequently intersected by numerous dolerite hill slopes [22]. Within the Brak River systems, ephemeral channels often form standing pools of water above the groundwater table, suggestive of a hydraulically connected system [22]. The dominant land use in the area is extensive livestock farming, mainly sheep and goats, which are well-suited to the semi-arid climate. The land cover is characterized by sparse vegetation, with grasslands and scrublands being the most common natural types. Irrigated agriculture is present but limited to areas with reliable groundwater and surface water resources.

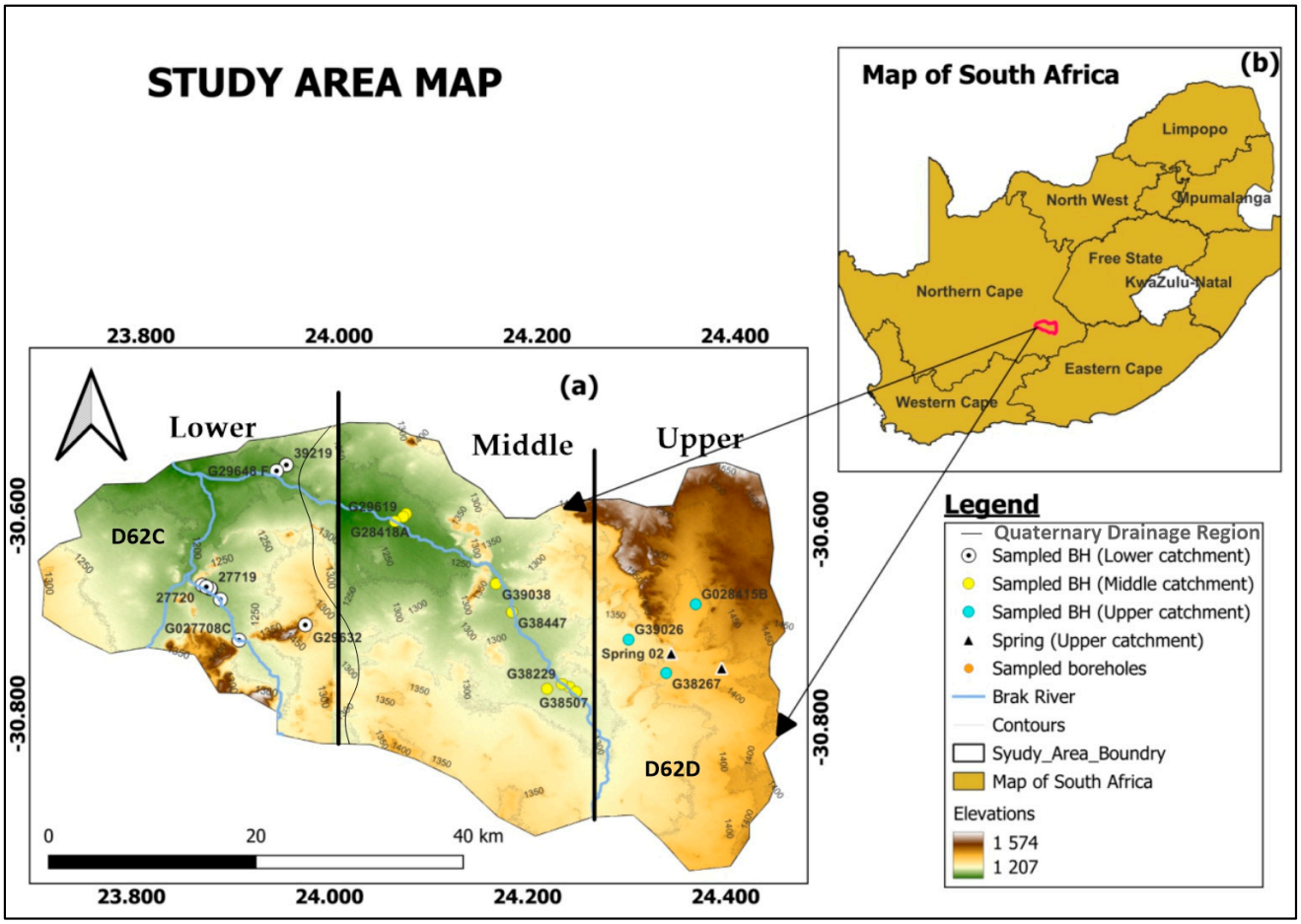

Figure 1. (**a**) The location of the study area with borehole sampling points drilled along the Brak River systems (solid line), contours (solid orange lines), and elevations (various colour coding). (**b**) The study area location with specific reference to the De Aar region, Northern Cape Province, South Africa [1].

2.2. Geology

The study area's geology comprises layered alluvium deposits of sand, clay, and silt that primarily cover the Brak River valley, as shown in Figure 2a. This alluvium deposit is subdivided into three to four layers: a thin layer of poorly sorted, highly heterogeneous

alluvium with flat rocks, fine to coarse sand, and fine to medium gravel on top of the fine silt sediments [23]. The western part of the study area contains most of the dolerite-intruded geological structures of the Ecca and Beaufort groups. Shale, mudstone, and flat-lying semi-permeable sandstone make up the bedrock [23]. Von Hoyer [24] states that the lower catchment contains substantial layers of fine-grained, light grey to greenish shale that alternate with sandstone, mudstone, and dolerite [21]. The alluvium deposit in the lower catchment is supported by the thick black shale and dolerite formation of the Ecca group [25]. Grey shale and light shale to whitish sandstone from the Beaufort group are interbedded in the high elevation of the middle and upper catchment [25]. Several deep boreholes were drilled through the shale at the lower catchment, and dolerite was struck at different depths (Figure 1a). This dolerite most likely comes from the still cropping that is present in the area [25]. Two common ring-shaped dolerites that are dark grey to black, fine to medium-grained, and extremely hard, with curved outcrops that overlap up to 30 m, exist in the study area [26]. The attributes of aquifers in Karoo sedimentary rock and dolerite are mostly due to fractures, which are mostly limited to shallow weathering zones that typically do not go deeper than 10 to 15 m [21].

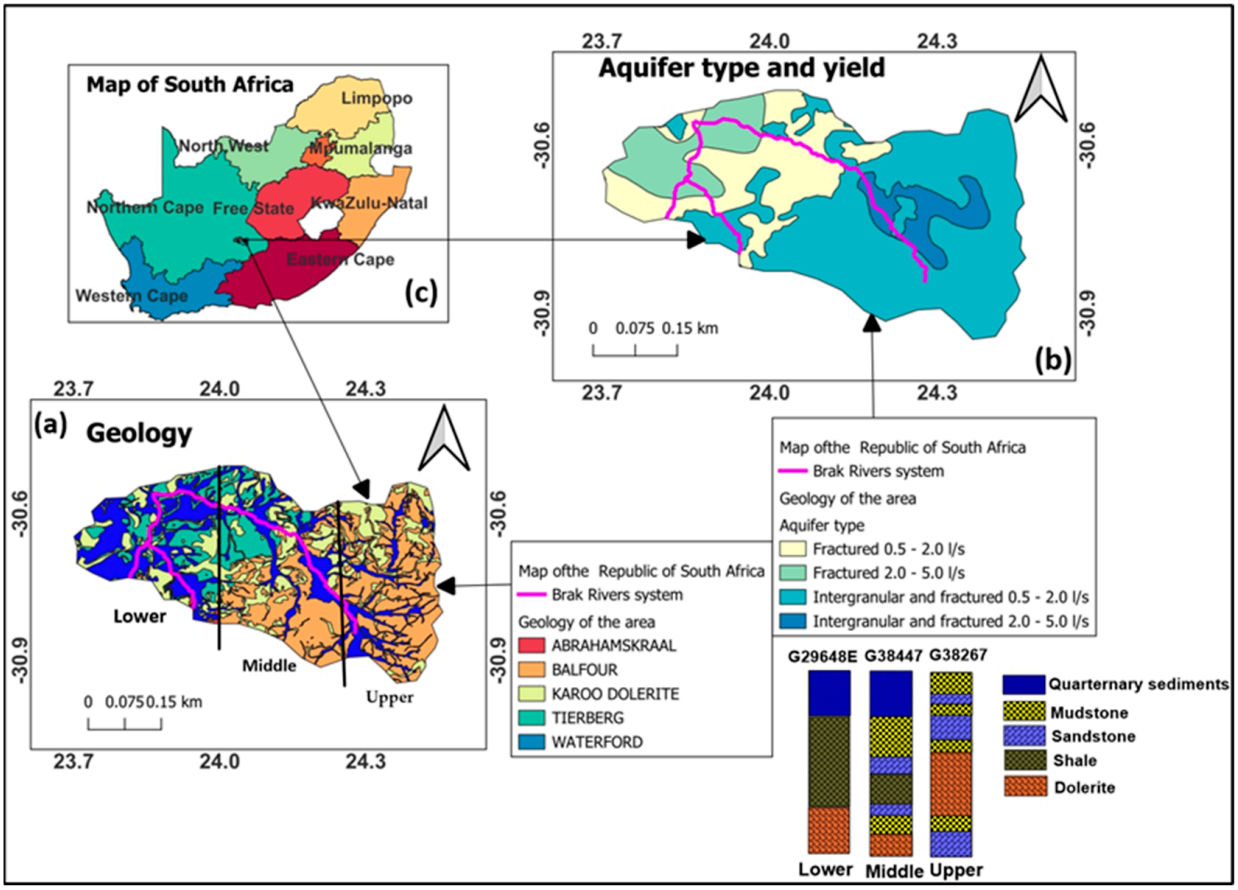

Figure 2. (**a**) Surface geology represented by Tierberg and Middleton's formation, which is composed of shale (olive drab), sandstone(electric blue), and mudstone (yellow), as well as Quaternary sediment of calcrete, sand, silt, clay, and gravel (blue). (**b**,**c**) Aquifer characteristics and the associated yields with specific reference to the De Aar, Northern Cape Province, South Africa [26].

2.3. Hydrogeology

A large portion of the study area (De Aar) is underlain by Karoo fractured aquifers, from which local communities rely exclusively for groundwater supply, despite generally low borehole yields of less than approximately 2 L/s [27]. Their storage capacity is low,

ranging from 0.0000297 to 0.000185 in confined aquifers, and 0.01 to 0.3 in unconfined aquifers, primarily due to elastic compression and gravity drainage, respectively [26]. Figure 2b illustrates the aquifer types and yields associated with each aquifer type. Each layer's thickness rapidly fluctuates, ranging from 5 to 15 m [23]. According to Vegter [21], these aquifers generally have low hydraulic conductivity, low transmissivity, and low yield, less than 1 L/s. Baloyi et al. [26] found slightly different results, with the transmissivity ranging from moderate to high up to 600 m^2/day, in highly fractured zones. Despite these challenges, wellfields are sometimes able to supply substantial volumes of groundwater, meeting the daily drinking water needs of towns, industries, and farms. High recharge occurs at higher elevations where rainfall infiltrates the subsurface, after which groundwater flows from the upper to the lower catchment through connected fractured aquifers. Where the topography drops to below the groundwater table or where a confining layer forces the flow to the surface, groundwater discharges as a spring. The borehole depth ranges from 5 to 60 m, a yield of 0.5 to 5.0 L/s, and the depth to static water level ranges from 3.32 to 4.77 m, as well as water strike ranging from 5.5 to 41 m (Figure 2b). This aquifer is greatly impacted by fluctuations in water levels brought on by excessive pumping from various users. Vegter [21,22] further classified the groundwater quality as class II, with the electrical conductivity (EC) ranging between 150 and 250 mS/m in the alluvium formation, and the total dissolved solids (TDS) greater than 1000 mg/L. Woodford [28] reported that the groundwater's electrical conductivity in the alluvium formation is 10–15% greater than that of the bedrock.

3. Materials and Methods

3.1. Groundwater Sampling Procedure

The groundwater sampling campaign was conducted across both unconfined and confined aquifer systems. Groundwater samples were collected to represent depth-specific conditions down the borehole profile under both ambient conditions [29]. A total of 26 boreholes were identified and sampled between 15 and 22 June 2025 for the analysis of hydrogeochemistry, stable isotopes, tritium, and radon activity from the unconfined and confined aquifer systems. The 26 boreholes were selected based on their distribution across the unconfined and confined aquifer systems to ensure representative spatial coverage and adequate characterization of hydrogeochemical and isotopic variability within a delineated aquifer system [1]. Of the 26 groundwater samples, 14 samples were from the unconfined aquifer and 12 samples from the confined aquifer, including two spring discharge samples. Before sampling, background information on each borehole was reviewed. All boreholes were recorded in the National Groundwater Archive (NGA); however, some were abandoned in the field with no regular maintenance. After purging for 10–20 min to remove stagnant water, field parameters pH and electrical conductivity (EC) were measured in the field using a calibrated YSI Model Pro1030 manufactured by —a Xylem Inc. in Yellow Springs, Ohio, and assembled in the United States of America, (USA). Total dissolved solids (TDS) were then estimated from the measured EC values using empirical relationships. Samples were collected in 500 mL and 250 mL sterilized plastic bottles using a depth-specific sampler and a submersible pump set at a reduced flow rate to allow low-disturbance pumping conditions and to minimize agitation and radon degassing. A depth-specific sampler designed to represent the water chemistry of distinct lithological zones was carefully lowered vertically to the target depth using a marked cable. Samples were collected directly from the pump discharge and stored in a cooler box filled with ice packs. Samples for radon were capped immediately and sealed with parafilm for in situ analysis. Each sampling bottle was rinsed three times with groundwater from the respective borehole before being filled with the sample. The bottles were then labelled

with the site code, date, and time of collection using a permanent marker. Groundwater samples in 500 mL bottles were transported to the South African National Standards (SANS)-accredited laboratory at Stellenbosch University for hydrogeochemical and stable isotope analyses. Samples for tritium analysis were transported to iThemba Isotopes Laboratory at the University of Witswatersrand, Johannesburg, South Africa.

3.2. Groundwater Analysis

3.2.1. Hydrogeochemical Analysis

The ion chromatography instrument was used to measure the concentrations of cations (Na, K, Ca, Mg) and anions (Cl, SO_4, $CaCO_3$, HCO_3) in the groundwater samples. All calibration solutions were prepared using ultrapure water (18.2 MΩ.cm) obtained using a Milli-Q Direct 16 system manufacture by Merck Millipore often branded as MilliporeSigma in the U.S. and Canada. Before analysis, a 15 mL sample was filtered using a 0.45 µm Nylon syringe filter. Based on the conductivity (EC in µS/cm) values of the samples, all samples were auto-diluted using ultrapure water on a Metrohm 858 autosampler, manufactured by Metrohm AG in Herisau, Switzerland, so that the conductivity was below 1000 µS/cm before injection. The analytical precision for major cations was acidified to 2% final acid concentration using ultra-pure HNO_3. The ionic balancing errors were calculated and found to be within ±5% [30]. Particulates were left to settle out before analysis. The results obtained are therefore a dissolved fraction of the sample. After auto-dilution, the samples were prefiltered through an inline auto-filtration cell equipped with a 0.22 µm cellulose filter. Subsequently, a 20 µL aliquot was injected for anion analysis. The anion mobile phase, consisting of 8 mM Na_2CO_3 and 0.25 mM $NaHCO_3$, was delivered at a flow rate of 0.8 mL/min, with the column temperature maintained at 30 °C. The descriptive statistics, which included minimum, maximum, mean, and standard deviation, for each variable, were calculated using Microsoft Excel 2019. Piper diagrams were generated with Geochemist Workbench (GWB) version 17.0 software to classify the water type within the study area. The Gibbs diagram analysis plot was used to identify the dominant processes controlling groundwater chemistry [31]. The quality assurance of the major cation and anion groundwater chemistry data was assessed by calculating the percent Ionic Charge Balance Error (ICBE) following the Ghosh and Jha [32] approach. The methods measure the possible mistakes that may have occurred during the field sampling campaign or laboratory assessment.

$$\text{Percent ICBE} = \frac{\sum\text{Cations} - \sum\text{Anions}}{\sum\text{Cations} + \sum\text{Anions}} \times 100\% \quad (1)$$

where 'Percent ICBE' = Ionic Charge Balance Error percentage; and the concentrations of all major cations and anions are expressed in milligrams per litre (Mq/L). Any value of 'Percent ICBE' < 10% provides proof that the water quality data is reliable, whereas data with 'Percent ICBE' > 10% should be eliminated from the analysis. The ICBE values of the groundwater samples in this study were ±5%; therefore, all were considered for the analysis. The analytical precision for major cations was acidified to 2% final acid concentration using ultra-pure HNO3.

3.2.2. Stable Isotopes

The groundwater samples were analysed for their 18O and 2H isotope ratios using the LGR T-LWIA-45-EP liquid water isotope analyser, which contains the laser analysis system, manufactured by Los Gatos Research (LGR) in San Jose, California, US. During preparations, a 1.9 mL filtered liquid sample was transferred to a 2 mL glass vial and closed with a PTFE septum cap. Samples were filtered using a 0.22 µm cellulose acetate syringe.

The analytical precision was estimated at 0.5‰ for 18O and 1.5‰ for 2H. Each standard or unknown was individually measured with 9 injections. The first four injections were ignored, and the results for the last 5 injections from each vial were averaged. The analytical results are presented in the common delta-notation:

$$\delta = \frac{R_{sample-}\ R_{standard}}{R_{standard}} \times 100\% \quad (2)$$

where R_{sample} and $R_{standard}$ are the stable isotopic ratios of oxygen and deuterium of the groundwater samples and the standard concentration, respectively. The measurements were presented in permille‰ relative to the Standard Mean Ocean Water (SMOW) of calibration standards. The isotope data were then plotted along the global meteoric water line (GMWL) of Craig; δ2H = 8δ18O + 10 [33], and the Kuruman local meteoric water line (LMWL) of Eddy Wyk; δ2H = 8δ18O + 10 [34]. The data quality control (QC) was ascertained by repeating 10% of the samples up to a maximum of 4 times equals to 40 samples, and confirming that deviations remained within the analytical uncertainty range [35].

3.2.3. Tritium Analysis

Tritium (^{3}H), with a half-life of 12.32 years, is widely used to date young and old groundwater. Concentrations are expressed in tritium units (TU), where 1 TU equals 1 ^{3}H atom per 10^{18} hydrogen atoms [36]. Atmospheric tritium was 1–10 TU before 1953 but rose sharply during 1953–1964 nuclear testing, while pre-1952 groundwater likely contained only 0.1–0.4 TU [16,36]. The tritium concentration level in groundwater and the rainfall samples was determined at the iThemba Environmental Isotopes Laboratory in the University of Witwatersrand, Johannesburg. The samples were distilled and subsequently enriched by electrolysis. The electrolysis cell consists of two concentric metal tubes, which are insulated from each other. The outer node, which is also a container, is of stainless steel. The inner cathode is of mild steel with a special surface coating. Next, 500 mL of the groundwater sample, having been first distilled and containing sodium hydroxide, is introduced into the cell. After several days, the electrolyte volume is reduced to 20 mL. The volume reduction of approximately 25 times produces a corresponding tritium enrichment factor of about 20. Samples of standard known tritium concentration were run in one cell of each batch to check on the enrichment attained. For liquid scintillation counting, samples were prepared by directly distilling the enriched water sample from the now highly concentrated electrolyte [37]. An amount measuring 10 mL of the distilled water sample is mixed with 11 mL Ultima Gold and placed in a vial in the analyser, and counted 2 to 3 cycles of 4 h [18]. The method has a detection limit of 0.3 TU for enriched samples [18]. The tritium apparent age of the groundwater was calculated using the tritium dating formula, following the approach by Bethke and Johnson [19], which is given as:

$$\tau = \frac{1}{\lambda} \ln\left[\left(\frac{\mathrm{No}}{\mathrm{N}}\right)\right] \quad (3)$$

where N is the measured tritium concentration in the groundwater sample, N_o is the natural background tritium concentration activity (groundwater recharge rainfall), τ is the groundwater age in years, and λ is the radioactive decay constant for tritium. Following the work of Allen and Boutt [36] on the crystalline fractured-rock aquifer of Tobago (West Indies), this study adopted 0.9 TU as the atmospheric background tritium level, derived from raw rainfall sample data in the study area. It was also assumed to be the threshold of the recently recharged groundwater from rainfall within the last few decades, typically after 1950. This means that all groundwater samples above this threshold are interpreted as recently recharged, young groundwater, or mixed with short residence times. In contrast,

samples below the threshold represent regionally recharged, older groundwater or mixed with longer residence times.

3.2.4. Radon Analysis

The RAD7 with RAD-H_2O accessory, manufactured in the in the Billerica, Massachusetts state, USA by Durridge Company, Inc., was used to determine radon concentration levels in groundwater samples. A desiccant within the RAD7 unit was used to reduce relative humidity (RH), as elevated RH can decrease detection efficiency. Until the radon concentration balance between the water and air is reached, the circulating air, which enters the water sample through a bubble stone fastened to the end of the inlet tube, removes radon from the water sample [38]. Before analysis, the detector was purged for 10–20 min to lower the relative humidity (RH) and to eliminate residual radon from earlier analyses [39] (Figure 3). Depending on relative humidity levels, either open- or closed-loop purging was applied to achieve a target relative humidity of approximately 10% (Figure 3). Blank analyses using distilled water confirmed a negligible detector background [40]. A radon-in-air monitor was used to measure the radon concentration in the air loop once equilibrium had been attained [38]. The time elapsed between sample collection and analysis was less than one hour, representing less than 10% of radon's half-life (3.82 days). Therefore, radioactive decay during sample handling was considered negligible, and no decay correction factor was applied [41]. Radon was transferred from water to air by bubbling air during analysis, and the equilibrium was established after five minutes, followed by a five-minute decay period [42]. The statistical uncertainty associated with radon concentration values (reported in Bq/L) is also recorded during analysis [41].

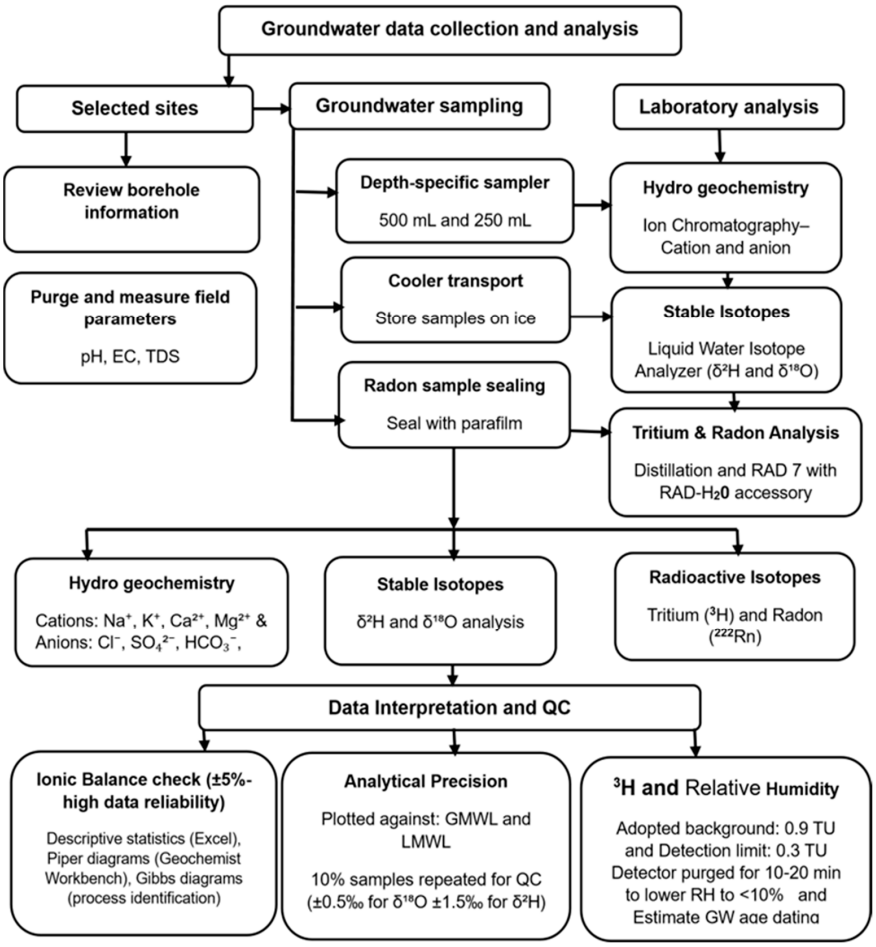

Figure 3. Methodological flowchart.

4. Results

4.1. Descriptive Statistical Analysis

Descriptive statistics for the physicochemical parameters of groundwater samples are summarized in Table 1. In the unconfined aquifer, the average major ion concentrations follow the order Na > Ca > Mg > K for cations and Cl > HCO_3 > SO_4 for anions, reflecting Na- and Cl-dominance in the water. Similarly, in the confined aquifer, the average ionic concentrations are ordered Na > Mg > Ca > K for cations and Cl > HCO_3 > SO_4 for anions, also confirming Na and Cl as dominant ions. Parameters exceeding the permissible limits set by the South African National Standard 241:2015 (SANS 241:2015) are bolded in dark black in Table 1. Electrical conductivity (EC) and total dissolved solids (TDS) in the unconfined aquifer range from 78.30 to 783.20 mS/m and 46.98 to 469.2 mg/L, with mean values of 221.41 mS/m and 132.85 mg/L, and standard deviations of 217.48 mS/m and 130.49 mg/L, respectively. In the confined aquifer, EC ranges from 7.61 to 777.10 mS/m and TDS from 4.57 to 466.26 mg/L, with averages of 189.67 mS/m and 113.80 mg/L, and standard deviations of 245.83 mS/m and 147.50 mg/L, respectively. On average, EC is higher in the unconfined aquifer than in the confined aquifer, with both exceeding the recommended maximum allowable limit of ≤170 mS/m. However, TDS values in both aquifers remain within the permissible limit of ≤1200 mg/L as per SANS 241:2015, classifying the water as fresh. Similarly, pH values in the unconfined aquifer range from 6.96 to 8.05, with a mean of 7.44 and a standard deviation of 0.33, typically of neutral to near-alkaline water. In the confined aquifer, pH values range from 6.45 to 8.37, averaging 7.20 with a standard deviation of 0.60, reflecting slightly acidic to moderately alkaline conditions. The average cation concentrations in the unconfined aquifer are 287.86 mg/L for Na, 61.62 mg/L for Ca, 55.76 mg/L for Mg, and 1.20 mg/L for K, with standard deviations of 345.17, 36.46, 61.25, and 0.87, respectively. In the confined aquifer, average concentrations are 266.08 mg/L (Na), 68.67 mg/L (Ca), 87.57 mg/L (Mg), and 1.79 mg/L (K), with corresponding standard deviations of 398.50, 27.43, 100.01, and 0.84. For anions, the unconfined aquifer exhibits average concentrations of 371.52 mg/L (Cl), 400.40 mg/L (HCO_3), and 274.77 mg/L (SO_4), with standard deviations of 30.68, 214.15, and 8.29, respectively. The confined aquifer shows average concentrations of 380.99 mg/L (Cl), 330.45 mg/L (HCO_3), and 224.52 mg/L (SO_4), with standard deviations of 660.96, 72.02, and 395.65, respectively. The concentrations of Na, Cl, HCO_3, and SO_4 in groundwater samples from both aquifers exceed the maximum permissible limits established by SANS 241:2015.

Table 1. Descriptive statistics of groundwater samples in unconfined and confined aquifers.

		Unconfined Aquifer				Confined Aquifer			
Parameters	**Limit**	**Min**	**Max**	**Ave.**	**STDEV**	**Min**	**Max**	**Ave.**	**STDEV**
pH	5 to 9.7	6.96	8.05	7.44	0.33	6.45	8.37	7.20	0.60
EC mS/m	≤170	78.30	**783.20**	**221.41**	**217.48**	7.61	**777.10**	**189.67**	**245.83**
TDS (mg/L)	≤1200	46.98	469.92	132.85	130.49	4.57	466.26	113.80	147.50
Na(mg/L)	≤200	71.28	**1239.42**	**287.86**	**345.17**	38.02	**1245.19**	**266.08**	**398.50**
Mg(mg/L)	≤150	19.91	246.70	55.76	61.25	21.22	301.24	87.57	100.01
K(mg/L)	≤100	0.19	3.21	1.20	0.87	0.60	3.05	1.79	0.84
Ca(mg/L)	≤200	9.07	143.01	61.62	36.46	33.37	107.03	68.67	27.43
Cl (mg/L)	≤300	42.48	**1819.23**	**371.52**	**494.95**	30.68	**1840.53**	**380.99**	**660.96**
SO_4 (mg/L)	≤250	43.79	**1360.75**	**274.77**	**371.12**	8.29	1364.44	224.52	**395.65**
HCO_3(mg/L)	≤300	**233.35**	**878.80**	**400.40**	165.99	**214.15**	**496.60**	**330.45**	72.02

4.2. Hydrogeochemistry Facies

Figures 4 and 5 present the Piper diagram showing the hydrogeochemistry of groundwater samples from unconfined and confined aquifers. The piper diagram classifies groundwater in an unconfined aquifer as Ca–HCO_3, Na–Cl, Na–K–HCO_3 mixed type, and Ca–Cl–HCO_3 mixed type (Figure 4). Similarly, the confined aquifer exhibits comparable facies, including Ca–HCO_3 water type, Na–Cl water type, Na–K–HCO_3 mixed water type, and Mg–Ca–Cl mixed water types (Figure 5). To further interpret the groundwater chemistry illustrated in the Piper diagram, the Gibbs diagram was employed, using the ratios $Na^+/(Na^+ + Ca^{2+})$ and $Cl^-/(Cl^- + HCO_3^-)$ plotted against total dissolved solids (TDS). Figure 6 illustrates the Gibbs diagram showing the geochemical processes controlling groundwater chemistry in both unconfined and confined aquifers. Samples from the unconfined aquifer are highlighted in red, those from the confined aquifer in green, and spring-discharge samples in purple. The results show that most groundwater samples plot within the rock dominance field in both unconfined aquifers and confined aquifers, with a Gibbs ratio $Na^+/(Na^+ + Ca^{2+}) > 0.5$ and $Cl^-/(Cl^- + HCO_3^-) < 0.5$. However, few samples in both aquifers plot towards the evaporation of precipitation dominance zone; meanwhile, the spring-discharge samples plot towards the low TDS precipitation-dominant field (Figure 6). The saturation indices (SI) of groundwater samples from both unconfined and confined aquifers were calculated using the PHREEQC version 3.4.0-12927 software package to understand mineral reactions in both aquifer systems. Figures 7 and 8 present mineral saturation in an unconfined and confined aquifer, while Figures 9 and 10 show the relationship between Na and Cl ions in both aquifer systems. The saturation indices (SI) for calcite, fluorite, gypsum, and halite were used to evaluate mineral–groundwater interactions in both unconfined and confined aquifers. SI values indicate whether groundwater is undersaturated (SI < 0), in equilibrium (SI = 0), or oversaturated (SI > 0) with respect to minerals. Results show that calcite and fluorite are generally oversaturated or near equilibrium, while gypsum and halite are undersaturated (Figures 7 and 8). Additionally, Na–Cl plots show strong positive correlations ($R^2 = 0.87$ in the unconfined aquifer and $R^2 = 0.97$ in the confined aquifer), with most samples plotting close to the 1:1 Na–Cl line, although some samples show deviations (Figures 9 and 10).

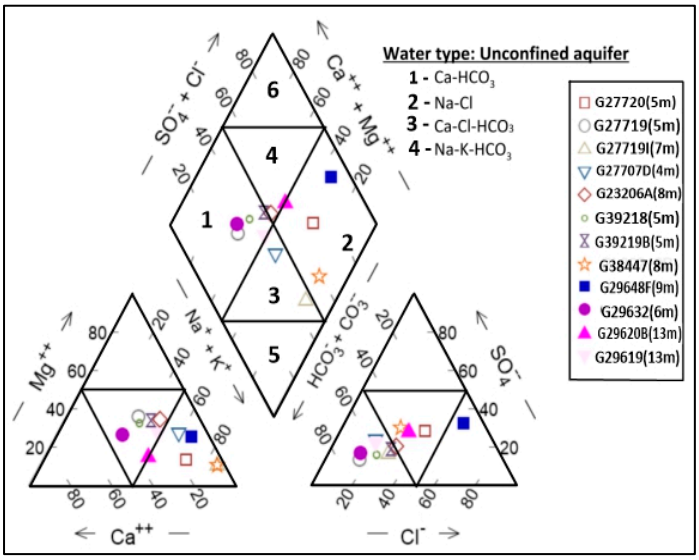

Figure 4. Hydrogeochemical facies in an unconfined aquifer.

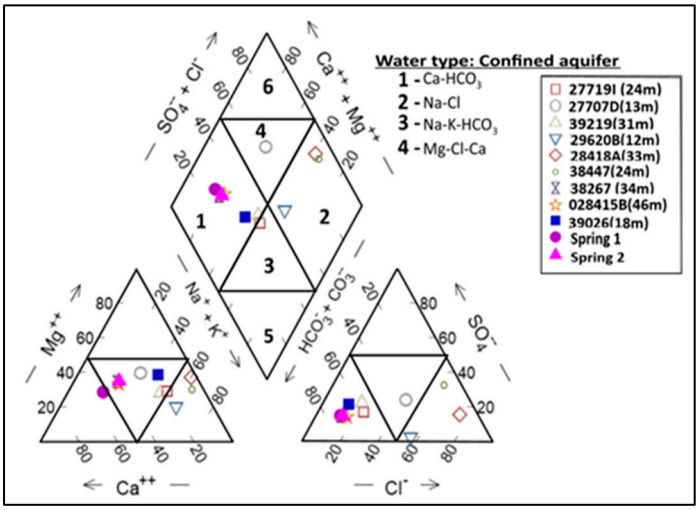

Figure 5. Hydrogeochemical facies in a confined aquifer.

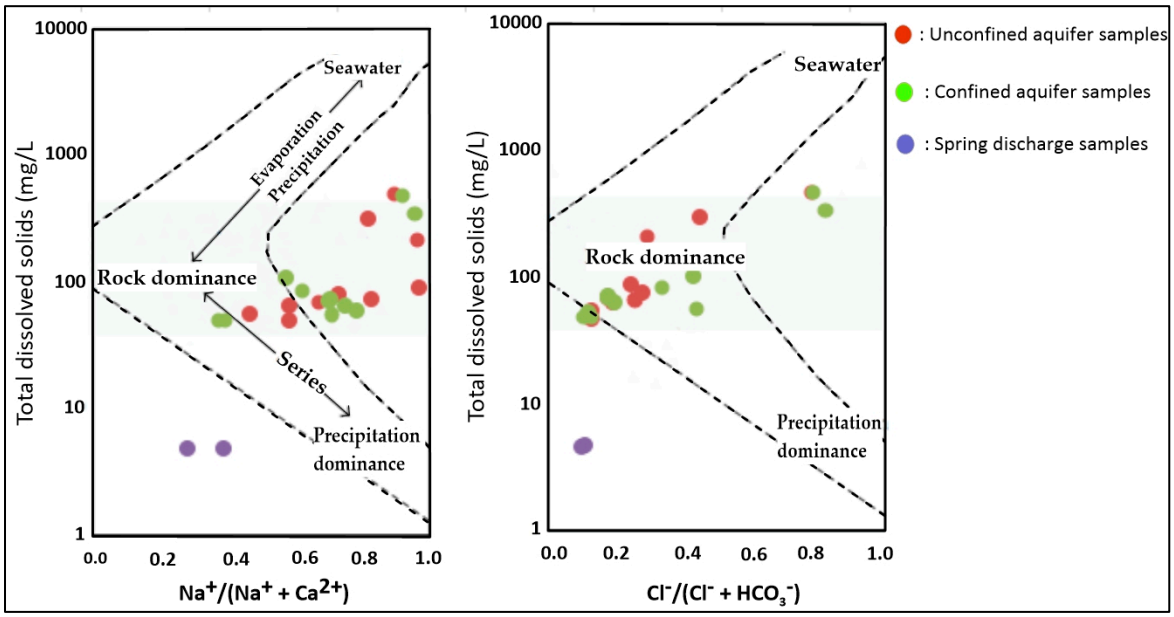

Figure 6. Gibbs diagram illustrating geochemical processes controlling groundwater chemistry in an unconfined and confined aquifer.

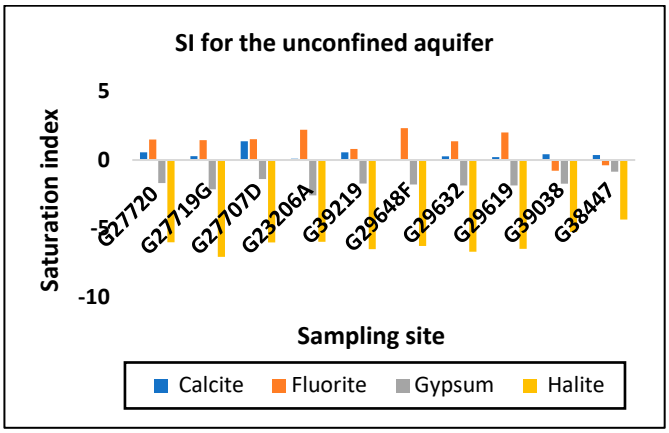

Figure 7. Mineral saturation in an unconfined aquifer.

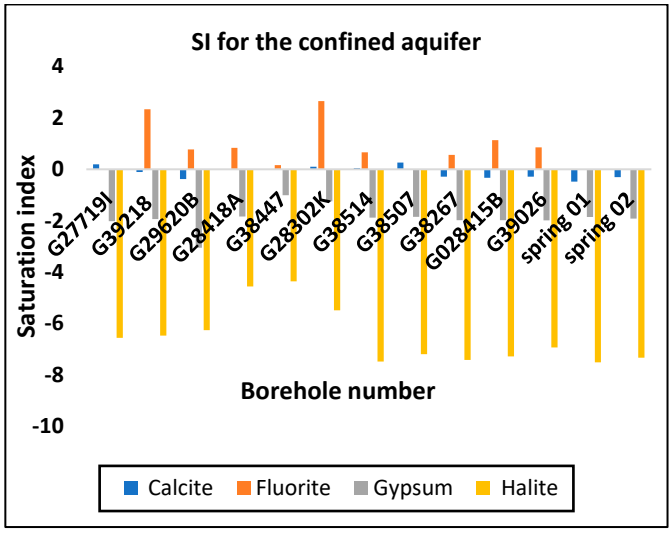

Figure 8. Mineral saturation in a confined aquifer.

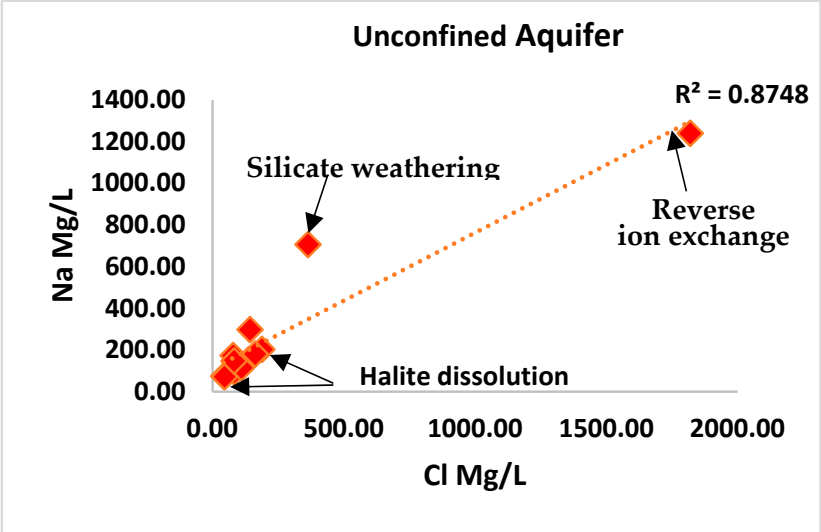

Figure 9. The ratio of Na/Cl in an unconfined aquifer.

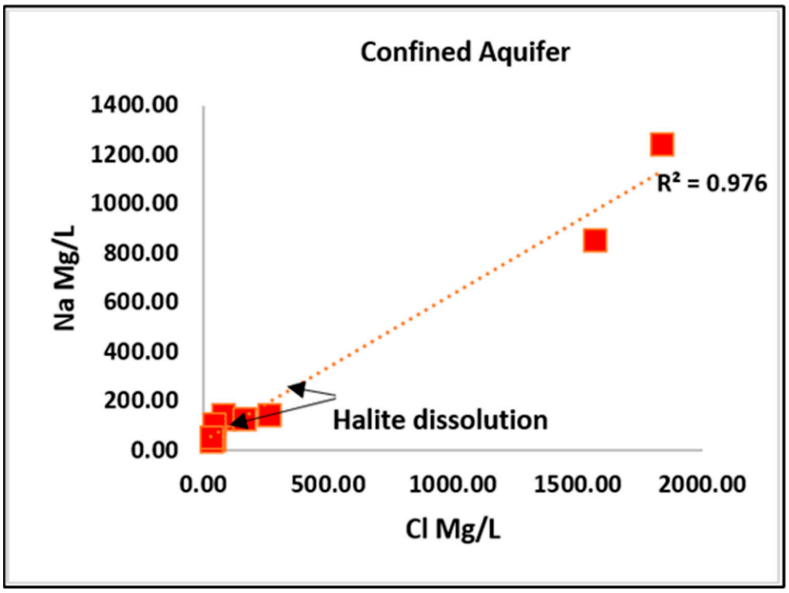

Figure 10. The ratio of Na/Cl in a confined aquifer.

4.3. Isotopes Analysis

Figure 11 shows the relationship between oxygen-18 and hydrogen-2 isotopes for the groundwater in both unconfined and confined aquifers, spring discharge, and rainfall samples. The plot shows that groundwater samples (both confined and unconfined) cluster close to the Global Meteoric Water Line (GMWL: $\delta^2H = 8\delta^{18}O + 10$) [43], and the Local Meteoric Water Line (LMWL: $\delta^2H = 5.58\delta^{18}O + 0.6$) [44]. This study recognizes the availability of previously established local meteoric water lines (LMWLs) in various regions of South Africa, including Cape Town and Pretoria. The Kuruman LMWL was selected for this study because of its similarity to the current study area. Groundwater samples from the unconfined aquifer displayed $\delta^{18}O$ values ranging from −4.84‰ to −2.44‰ and δ^2H values from −17.65‰ to −3.90‰, evaporatively enriched samples (Figure 10). In contrast, groundwater samples from the confined aquifer exhibited $\delta^{18}O$ values between −4.88‰ and −3.70‰ and δ^2H values between −33.11‰ and −21.86‰, isotopically depleted samples (Figure 10). The isotopic composition of spring discharge samples ranged from −4.09‰ to −3.69‰ for $\delta^{18}O$ and from −26.68‰ to −24.99‰ for δ^2H (depleted samples), whereas surface water samples showed $\delta^{18}O$ values of −3.68‰ to −3.58‰ and δ^2H values of −23.62‰ to −22.76‰, isotopically depleted samples (Figure 10). The isotopic composition of rainfall was −5.53‰ for $\delta^{18}O$ and −30.48‰ for δ^2H, shows more depleted signature compared to groundwater samples. The majority of groundwater samples from both the unconfined and confined aquifers plot below the Global Meteoric Water Line (GMWL), while a few samples, including spring discharges, show slight deviation. In contrast, rainfall samples plot on the lower end below the local meteoric water line (LMWL). The unconfined aquifer samples are relatively more isotopically enriched than those from the confined aquifer. The clustering of most samples along and below the meteoric water lines shows limited evaporation effects in both aquifer systems.

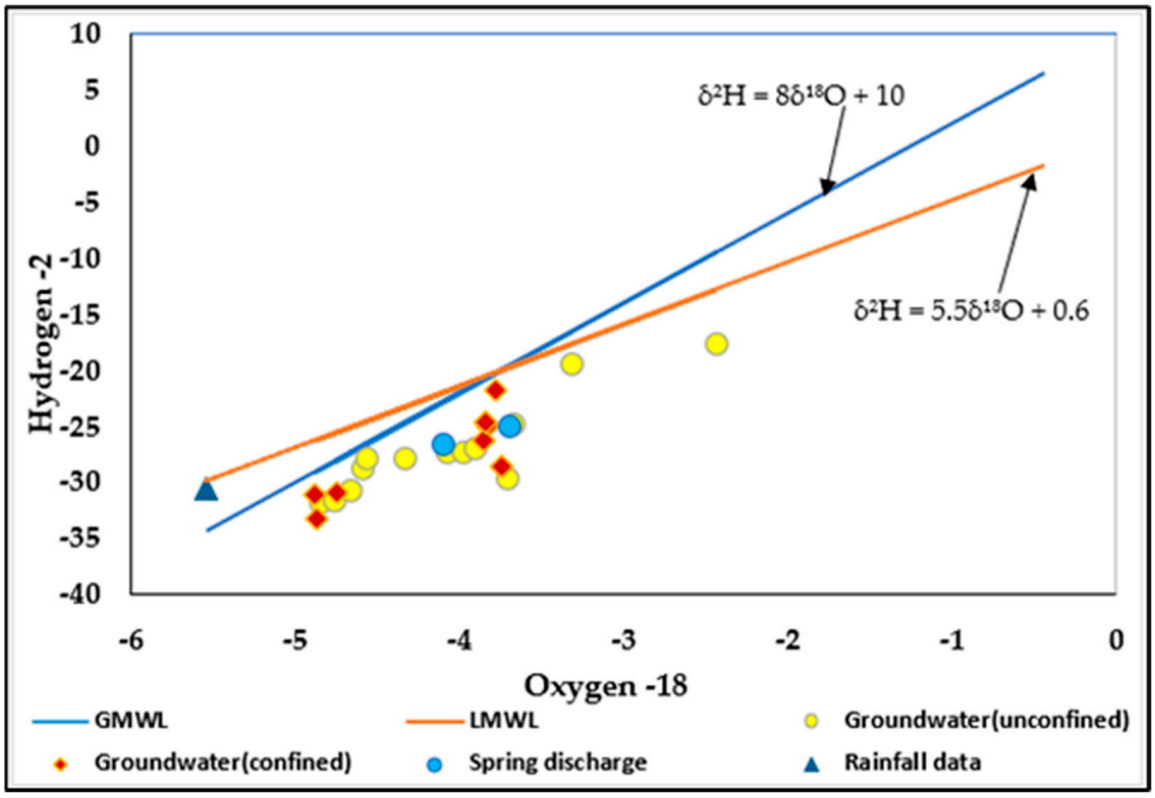

Figure 11. Relationship between δ^2H and $\delta^{18}O$ for groundwater in unconfined and confined aquifers, spring discharge, as well as the rainfall samples.

4.4. Environmental Tracers of Tritium (^{3}H) and Radon (^{222}Rn) Analysis

As previously stated, tritium greater than one (>1 TU) is interpreted as young, recently recharged groundwater with shorter residence time (<30 years), 0.5–1 TU mixed groundwater with intermediate residence time (30–50 years), and <0.5 old regional recharged groundwater with longer residence time (60–500 years). The use of tritium as a standalone tracer is well established in similar hydrogeological settings. In this study, tritium-derived ages are crosschecked against hydrogeochemical characteristics, providing indirect validation [18,45]. The unconfined aquifer samples show tritium values ranging from 0.2 to 1.4 TU, with apparent ages between 19 and 109 years (Table 2). In contrast, the confined aquifer shows tritium concentrations ranging from 0.1 to 1.4 TU, with apparent groundwater ages between 19 and 477 years. As tritium increases, the apparent groundwater age decreases significantly (Table 2). These results show a negative relationship between tritium concentration and apparent age, as illustrated in the graph (Figure 12). As expected, the unconfined aquifer shows moderate to high radon concentrations, particularly after purging the borehole (Figure 13). In contrast, groundwater from the confined aquifer also shows variable but generally high radon concentrations, particularly after purging (Figure 14). However, the distribution differs from that of the unconfined aquifer as expected.

Table 2. The tritium activity of groundwater samples with corresponding apparent age, and depth from both unconfined and confined aquifers.

Unconfined Aquifer					
Site ID	**Material Type**	**Depth**	**Sampling Depth**	**Tritium (TU)-Unconfined Aquifer**	**Apparent Age**
27720	Alluvium	40	5	0.2	109
27719G	Alluvium	13	4	1.3	20
23206A	Alluvium	22	7	0.7	38
39218	Alluvium	18	5	1.1	24
39219	Alluvium	36	5	0.7	39
29648F	Alluvium	23	9	0.7	36
29619	Alluvium	22	13	0.8	34
39038	Alluvium	13	7	1.4	19
38447	Alluvium	48	8	0.7	40
Confined aquifer					
Site ID		**Depth**	**Sampling depth**	**Tritium (TU)-Confined aquifer**	**Apparent Age**
27719I	Shale	45	24	0.8	32
27707D	Shale	12	10	1.4	19
39219	Mudstone	36	31	0.6	47
29620B	Dolerite	14	12	1.0	28
28418A	Shale	53	33	0.9	29
38447	Shale	48	24	0.1	477
38514	Mudstone	42	24	1.2	22
38507	Dolerite	42	36	0.8	32
38267	Dolerite	60	34	0.7	40
028415B	Mudstone	63	46	0.6	47
39026	Mudstone	42	18	1.4	19
Spring1	Mudstone			0.4	60
Spring2	Mudstone			1.1	24

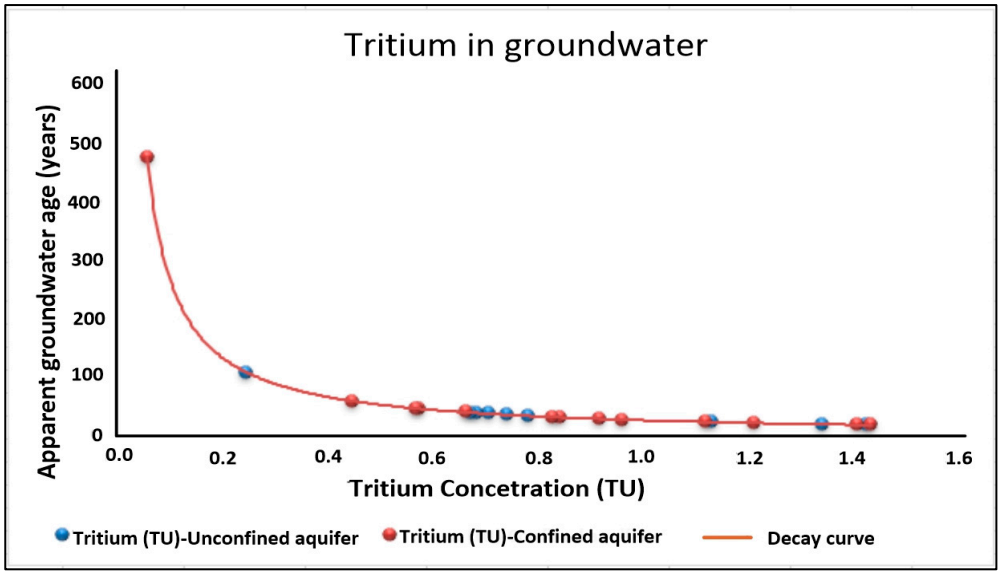

Figure 12. The exponential curve illustrating the background tritium in the atmosphere (threshold) and the decay period since the rainfall recharge isolated from the atmosphere.

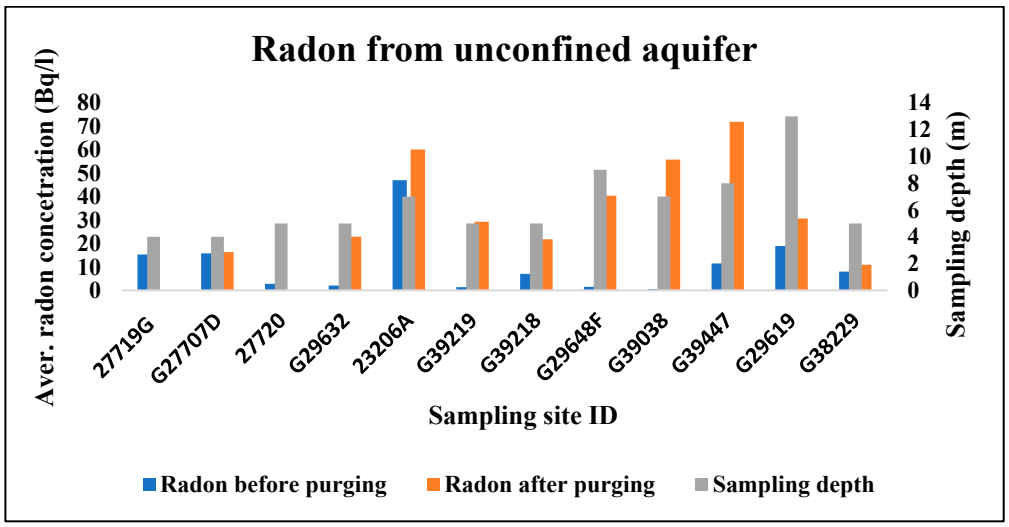

Figure 13. The distribution of radon (^{222}Rn) activity in groundwater from unconfined aquifers.

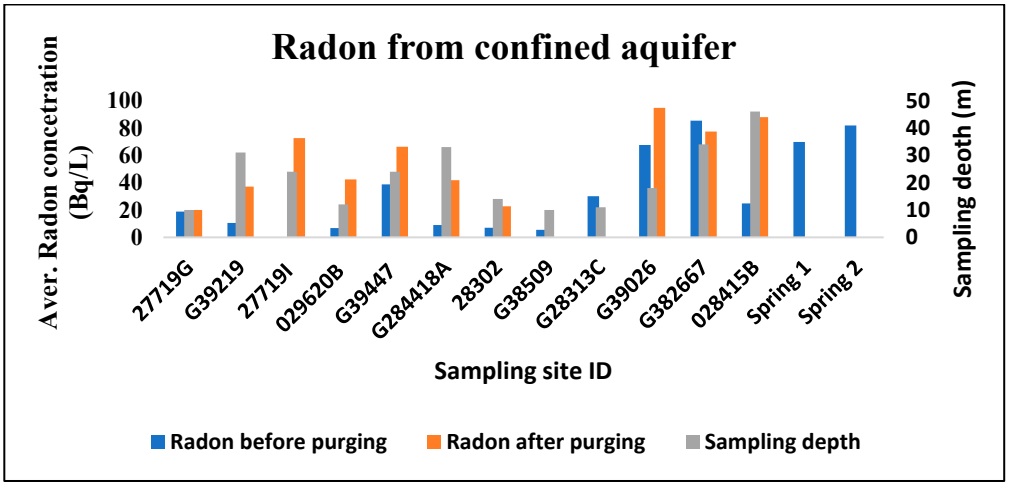

Figure 14. The distribution of radon (^{222}Rn) activity in groundwater from confined aquifers and spring discharges.

5. Discussion

5.1. Hydrogeochemical Processes and Water Type

Groundwater from both aquifers (unconfined and confined) generally exhibits elevated electrical conductivity (EC), but on average, falls within the limit, indicating great mineralisation and longer water–rock interaction with salinity-related concerns [46]. However, total dissolved solid (TDS) values remain within the freshwater classification of low mineralisation. These findings are consistent with observations by Vegter [22] in De Aar, Northern Cape, regarding an EC range of 150 to 250 mS/m, but inconsistent with their study, which reported TDS greater than 1000 mg/L. Similarly, Woodford [34] reported that groundwater within alluvial formations typically exhibits EC values 10–15% higher than those of adjacent bedrock aquifers, inconsistent with the patterns observed in this study. The groundwater facies in both unconfined and confined aquifers indicate that water–rock interaction, ion exchange, and mixing processes control groundwater evolution, with Ca–HCO_3 water suggesting local recent recharge influenced by carbonate mineral dissolution like shale; meanwhile, Na–Cl water indicates cation exchange between Cl and Na influenced by evaporation before or during infiltration linked with regional recharged groundwater [46]. Comparable hydrogeochemical evolution was documented by Adams et al. [47] in the basement aquifers of Namaqualand, where elevated salinity and Na–Cl dominance were linked to long groundwater flow paths and limited modern recharge. The Gibbs diagram further confirms that water–rock interaction, evaporation, and precipitation control groundwater chemistry, consistent with the Piper diagram results. Although samples from both aquifers (unconfined and confined) fall within the rock-dominance field, confirming water–rock interaction, low TDS values indicate shorter residence time with limited mineral interaction, a pattern associated with direct local recharge and a hydraulically connected system. Furthermore, the spring discharge plotting on the low TDS precipitation dominance field provides strong evidence of hydraulic connectivity between recharge zones and spring outlets. These results are consistent with findings by Gao et al. [31] and Akpah [47], who also identified rock–water interaction, mineral weathering, and dissolution as the primary controls on groundwater chemistry. The mineral saturation indices (SI) analysis further supports the Piper diagram and Gibbs diagram results, highlighting gypsum and halite dissolution as key processes controlling Na and Cl enrichment in groundwater [48]. The contribution of halite and gypsum dissolution to sodium enrichment observed in this study is consistent with findings by Ogwah and Eyankware [42], who reported similar salinity controls in comparable hydrogeological settings. However, the strong influence of water–rock interaction on recharge water contrasts with conclusions by Marandia and Shand [46], who suggested a lesser role for mineral dissolution processes. In contrast, studies by Lalumbe et al. [49] in the Soutpansberg region found that silicate weathering and fluorite dissolution, together with unstable evaporite minerals, are key contributors to groundwater salinity. Their contrast with the findings of this study may be attributed to various hydrogeological factors, including geological formation, climate variability, and recharge sources across the study areas.

5.2. Stable Isotopes

The clustering of groundwater samples closer to the GMWL and LMWL indicates that groundwater in an unconfined and confined aquifer system is primarily recharged by meteoric water (rainfall). This also confirms that rainfall infiltration is the main source of recharge water within the study catchment, aligning well with those found by Madlala et al. [50] and Yeh et al. [51]. Consistent with hydrogeochemistry results, the stable isotopes support the interpretation that recharge in both aquifer systems is directly linked to local and regional rainfall events. The isotopic similarities between rainfall, groundwater, and

spring discharge samples further confirm hydraulic connectivity between the recharge and discharge zones [52,53]. Slight deviations below the meteoric water lines suggest evaporative enrichment before infiltration, likely occurring in surface water bodies or soil moisture before recharge. Similar to findings by Steyl et al. [12] in the Modder River catchment, groundwater recharge was shown to be predominantly meteoric with minimal evaporative enrichment. Their interpretation aligns with the conceptual framework proposed by Clark and Fritz [13], who demonstrated that isotopically enriched groundwater often reflects evaporation or focused recharge, while depleted signatures are associated with diffuse rainfall recharge under cooler or higher-altitude conditions. Comparable isotopic trends were also reported by Leketa et al. [52] in fractured bedrock aquifers of Johannesburg, where depleted isotopic compositions were linked to recharge from higher-elevation rainfall.

5.3. Tritium Concentration (^3H)

Tritium was used to distinguish between young and old groundwater, based on its introduction to the hydrological cycle during atmospheric nuclear testing between 1951 and 1964 [13,16,36]. Higher tritium values (>1 TU) in the unconfined and confined aquifer correspond with relatively fresh groundwater chemistry, indicating young recent recharge (>30 years) likely through infiltration of rainfall, and limited geochemical evolution [16]. On the other hand, a moderate tritium range between 0.5 and 1 TU indicates a hydraulically connected system representing intermediate groundwater ages, typically between 30 and 50 years [16]. In contrast, lower tritium values (<0.5 TU) in the confined aquifer correspond to higher mineralization, indicating old groundwater (60–109 years) likely recharged through regional rainfall from high-altitude areas with longer residence times, and stronger rock–water interaction [16]. These interpretations are consistent with the tritium-based age classification framework proposed by Clark and Fritz [13], which associates measurable tritium with post-1950s recharge and low or absent tritium with pre-1950s recharge or mixed groundwater. Although Tritium indicates relatively young groundwater, the Gibbs Diagram shows that groundwater chemistry in both aquifer systems is mainly controlled by rock–water interaction. This apparent contrast suggests that recharge water acquires dissolved ions through mineral dissolution during infiltration. Results from Radon-222 further support this interpretation, as higher radon concentrations after purging indicate groundwater originating from the aquifer formation after interacting with uranium-bearing minerals in the aquifer matrix. For example, Tye et al. [54] recorded radon activities exceeding 50 Bq/L in igneous terrains, attributing these values to uranium-rich lithologies and fracture-controlled groundwater circulation. The observed contrast in radon concentrations between the unconfined and confined aquifers in the present study, therefore, reflects differing degrees of rock–water interaction and supports the presence of complex recharge pathways and hydraulic connectivity between aquifer units. Comparable interpretations were reported by Strydom et al. [29] and Eilers et al. [41] in fractured-rock aquifers of the Karoo, where elevated radon concentrations were linked to deeper groundwater circulation, fracture-controlled flow, and mixing between shallow and deeper aquifer systems. In particular, Strydom et al. [29] observed substantial increases in radon activity following borehole pumping, demonstrating that purging enhances the contribution of formation water, an observation fully consistent with the results of this study. Although Eilers et al. [41] reported higher radon values in some shallow groundwater settings, their findings similarly emphasized the role of regional flow contributions and structural controls on recharge. When considered alongside the stable isotope evidence, the radon results confirm the presence of a dual groundwater system characterized by vertical hydraulic connectivity and mixed recharge regimes. These findings further emphasize the need for aquifer-specific groundwater allocation and management strategies, prioritizing the protection of recharge

and spring-discharge zones and limiting abstraction from the confined aquifer to safeguard long-term groundwater allocation.

6. Implication of the Results to Groundwater Allocation

Hydrogeochemical facies and environmental tracers help identify groundwater recharge sources and provide a scientific basis for supporting groundwater allocation in groundwater-dependent communities. Groundwater with a Ca–HCO_3 water type generally is suitable for domestic water supply and agricultural use, adhering to the Department of Water Affairs water quality guidelines for irrigation and livestock watering [55] while Na–Cl-dominated groundwater type indicates higher salinity and may require blending with fresher water [4,46]. Areas dominated by rock–water interaction indicate relatively stable groundwater suitable for long-term groundwater allocation. However, evaporation dominance and halite or gypsum dissolution increase salinity and total dissolved solids (TDS), requiring controlled groundwater allocation [4]. The stable isotope composition shows that groundwater originates from meteoric recharge with limited evaporation, indicating a renewable resource if abstraction remains within recharge limits [22]. The isotopically enriched unconfined aquifer is more vulnerable to contamination and climate variability, while the depleted confined aquifer and spring discharge zones represent more protected groundwater reserves, requiring aquifer-specific management and protection of recharge zones [22]. Consistent with hydrogeochemistry and stable isotopes results, the tritium-derived groundwater ages and radon distribution show that the confined aquifer holds older groundwater that should be managed as a strategic reserve, taking into account its vertical hydraulic connectivity, while the unconfined aquifer contains relatively younger, recently recharged groundwater suitable for regular abstraction, in accordance with hydrogeochemistry and stable isotope results [16,34]. These findings provide important guidance for groundwater allocation and long-term water security in groundwater-dependent communities.

7. Conclusions and Recommendations

This study aimed to trace groundwater recharge sources and identify the hydrogeochemical and isotopic processes controlling groundwater quality within a delineated fractured aquifer system in De Aar, Northern Cape, South Africa. By integrating hydrogeochemistry, stable isotopes (δ^2H and $\delta^{18}O$), and environmental tracers (^3H and ^{222}Rn), the study sought to improve understanding of recharge mechanisms, groundwater evolution, and their implications for sustainable groundwater allocation in a semi-arid, groundwater-dependent catchment. The results demonstrate that the study successfully achieved its aim and objectives by providing a comprehensive characterization of both unconfined and confined aquifer systems within the study area. Hydrogeochemical analysis indicates that groundwater in both aquifers is primarily controlled by rock–water interaction, with additional influences from evaporation, ion exchange, and mineral dissolution. The dominance of Ca–HCO_3 and Na–Cl hydrogeochemical facies reflects groundwater evolution processes linked to carbonate weathering, evaporite dissolution (gypsum and halite), and cation exchange. Although electrical conductivity is relatively high, total dissolved solids remain within the freshwater range, indicating moderate mineralization. Stable isotope results confirm that groundwater in both aquifers is predominantly recharged by meteoric water, with rainfall infiltration identified as the primary recharge mechanism. The close similarity between rainfall, groundwater, and spring isotopic signatures highlights strong hydraulic connectivity between recharge and discharge zones, while slight isotopic enrichment indicates minor evaporation before infiltration. Environmental tracers further refine this understanding by distinguishing groundwater residence times and flow dynamics.

Tritium results indicate that the unconfined aquifer contains relatively young groundwater recharged within recent decades, whereas the confined aquifer stores older groundwater with longer residence times and stronger rock–water interaction. Radon-222 concentrations confirm active interaction between groundwater and aquifer materials, supporting fracture-controlled flow and mixing between shallow and deeper groundwater systems. Collectively, these findings reveal a dual groundwater system characterized by vertical hydraulic connectivity and mixed recharge pathways, thereby providing a robust scientific basis for groundwater allocation in the study area. The results emphasize the need to prioritize the protection of recharge and spring-discharge zones, regulate abstraction from the confined aquifer, and utilize the more actively recharged unconfined aquifer for regular supply, thereby supporting long-term groundwater security in groundwater-dependent communities. A key limitation of the study is its reliance on major ions and isotope tracers alone, which may not fully capture complex mixing processes, precise groundwater ages, detailed geochemical reactions, and spatial variability in recharge dynamics. Therefore, future research should integrate numerical and conceptual modelling approaches to enhance the understanding and interpretation of groundwater recharge sources, flow systems, and geochemical evolution.

Author Contributions: Conceptualization, L.B., S.M. and H.P.; methodology, L.B., S.M. and T.K.; software, L.B. and S.M.; validation, H.P. and T.K.; formal analysis, L.B.; investigation, L.B., T.K., H.P., S.M., and M.B.; resources, L.B., T.K. and H.P.; data curation, L.B. and S.M.; writing—original draft preparation, L.B.; writing—review and editing, M.B.M., S.M., T.K. and H.P.; visualization, L.B.; supervision, T.K. and H.P.; project administration, L.B.; funding acquisition, L.B., T.K. and H.P. All authors have read and agreed to the published version of the manuscript.

Funding: This research was funded by the National Department of Water and Sanitation, South Africa. The fieldwork was co-funded by the University of the Western Cape (UWC) and the Council for Scientific and Industrial Research (CSIR).

Data Availability Statement: The data presented in this study are available on request from corresponding authors due to privacy.

Acknowledgments: This paper forms part of the corresponding author's ongoing research. The authors gratefully acknowledge the National Department of Water and Sanitation, the University of the Western Cape, and the Council for Scientific and Industrial Research for their continued support. The authors also thank Madlala T., Makhetha J., Umunezero A.A., Mqhayi S., Zulu S.M., for their technical assistance and support during field investigations. The authors further appreciate the reviewers' valuable time and constructive comments on the manuscript.

Conflicts of Interest: The authors declare no conflicts of interest.

References

1. Baloyi, L.; Kanyerere, T.; Muchingami, I.; Pienaar, H. Application of Hydrogeophysical Techniques in Delineating Aquifers to Enhancing Recharge Potential Areas in Groundwater-Dependent Systems, Northern Cape, South Africa. *Water* **2024**, *16*, 2652. [CrossRef]
2. Li, F.; Song, X.; Tang, C.; Liu, C.; Yu, J.; Zhang, W. Tracing infiltration and recharge using stable isotope in Taihang Mt., North China. In *Environmental Geology*; Springer: Berlin/Heidelberg, Germany, 2007; pp. 687–696. [CrossRef]
3. Gong, Y.F.; Liu, X.; Ma, B.; Qi, P.F.; Li, Y. Using geochemistry and environmental tracers to study shallow unconfined aquifer recharge and mineralization processes in the Yinchuan Plain, arid Northwest China. *Hydrol. Res.* **2021**, *52*, 658–675. [CrossRef]
4. Chung, S.Y.; Rajendran, R.; Senapathi, V.; Sekar, S.; Ranganathan, P.C.; Oh, Y.Y.; Elzain, H.E. Processes and characteristics of hydrogeochemical variations between unconfined and confined aquifer systems: A case study of the Nakdong River Basin in Busan City, Korea. *Environ. Sci. Pollut. Res.* **2020**, *27*, 10087–10102. [CrossRef]
5. Adams, S.; Titus, R.; Pietersen, K.; Tredoux, G.; Harris, C. Hydrochemical Characteristics of Aquifers Near Sutherland in the Western Karoo, South Africa. Available online: www.elsevier.com/locate/jhydrol (accessed on 19 December 2019).

6. Kumar, M.; Ramanathan, A.; Keshari, A.K. Understanding the extent of interactions between groundwater and surface water through major ion chemistry and multivariate statistical techniques. *Hydrol. Process.* **2009**, *23*, 297–310. [CrossRef]
7. Glover, E.T.; Akiti, T.T.; Osae, S. Environmental Stable Isotope Studies of Groundwater in the Accra Plains. 2016. Available online: www.elixirpublishers.com (accessed on 30 September 2025).
8. Huang, T.; Pang, Z. The role of deuterium excess in determining the water salinisation mechanism: A case study of the arid Tarim River Basin, NW China. *Appl. Geochem.* **2012**, *27*, 2382–2388. [CrossRef]
9. Weaver, J.M.C.; Talma, A.S.; Cave, L.C. *Geochemistry and Isotopes for Resource Evaluation in the Fractured Rock Aquifers of the Table Mountain Group*; Water Research Commission: Pretoria, South Africa, 1999.
10. Dansgaard, W. Stable isotopes in precipitation. *Tellus A Dyn. Meteorol. Oceanogr.* **2012**, *16*, 436. [CrossRef]
11. Leketa, K.; Abiye, T.; Butler, M. Characterisation of groundwater recharge conditions and flow mechanisms in bedrock aquifers of the Johannesburg area, South Africa. *Environ. Earth Sci.* **2018**, *77*, 727. [CrossRef]
12. Gomo, M.; Steyl, G.; Van Tonder, G. Investigation of Groundwater Recharge and Stable Isotopic Characteristics of an Alluvial Channel. *J. Waste Water Treat. Anal.* **2012**, *s12*, 1–7. [CrossRef]
13. Clark, I.D.; Fritz, P. *Environmental Isotopes in Hydrogeology*; CRC Press: Boca Raton, FL, USA, 2013. [CrossRef]
14. Adomako, D.; Gibrilla, A.; Maloszewski, P.; Ganyaglo, S.Y.; Rai, S.P. Tracing stable isotopes (δ2H and δ18O) from meteoric water to groundwater in the Densu River basin of Ghana. *Environ. Monit. Assess.* **2015**, *187*, 1–15. [CrossRef] [PubMed]
15. Benjamin, L.; Knobel, L.L.; Hall, L.F.; Cecil, L.D.; Green, J.R. *Development of a Local Meteoric Water Line for Southeastern Idaho, Western Wyoming, and South-Central Montana*; No. 2004-5126; U.S. Geological Survey (USGS): Reston, VA, USA, 2005.
16. Gilmore, T.; Cherry, M.; Gastmans, D.; Humphrey, E.; Solomon, A.D.K. The 3h/3he Groundwater Age-Dating Method And Applications. *Derbyana* **2021**, *42*, e740. [CrossRef]
17. Zhao, Z.; Wang, D.; Bai, Y.; Yan, C.; Xu, X. Research on Establishing Tritium Concentration Model of Precipitation in Northeast of Tarim Basin Based on Factor Analysis. In *IOP Conference Series: Earth and Environmental Science*; Institute of Physics Publishing: Bristol, UK, 2019. [CrossRef]
18. Telloli, C.; Rizzo, A.; Salvi, S.; Pozzobon, A.; Marrocchino, E.; Vaccaro, C. Characterization of groundwater recharge through tritium measurements. *Adv. Geosci.* **2022**, *57*, 21–36. [CrossRef]
19. Bethke, C.M.; Johnson, T.M. Groundwater age and groundwater age dating. *Annu. Rev. Earth Planet. Sci.* **2008**, *36*, 121–152. [CrossRef]
20. van Niekerk, L.; Adams, J.; Lamberth, S.J.; Taljaard, S. *Determination of Ecological Water Requirements for Surface Water (River, Estuaries and Wetlands) and Groundwater in the Lower Orange WMA. Buffels, Swartlintjies, Spoeg, Groen, and Sout Estuaries Ecological Water Requirement*; RDM/WMA06/00/CON/COMP/0316; South African Department of Water and Sanitation (DWS): Pretoria, South Africa, 2017.
21. Vegter, J.R. Evaluation of an Alluvial Aquifer at Caroluspoort, De Aar, South Africa. Department of Water Affairs Pretoria. 1975_GH2828. Available online: https://www.dws.gov.za/ghreport/Home/Result.aspx?Search=%20FORMSOF%20(INFLECTIONAL,%20gh2828) (accessed on 17 December 2025).
22. Vegter, J.R. De Aar's Groundwater Supply: A Digest of the Past and an Outlook for the Future. Department of Water Affairs-Pretoria. 1992_GH3775. Available online: https://www.dws.gov.za/ghreport/Home/Result.aspx?Search=%20formsof%20(inflectional,%20gh3775) (accessed on 9 December 2025).
23. Van Wyk, E. Application of Preussag-Type Screens in Groundwater Investigation in the Northern Area, De Aar. Department of Water-Pretoria. 1989_GH3673. Available online: https://www.dws.gov.za/ghreport/Home/Result.aspx?Search=%20FORMSOF%20(inflectional,%20gh3673) (accessed on 12 January 2026).
24. Von Hoyer, M.E. A Groundwater Survey of the Burgerville, Zewefontein Area, De Aar, Cape Province. Department of Water Affairs-Pretoria. 1976_GH2886. Available online: https://www.dws.gov.za/ghreport/Home/Result.aspx?Search=%20FORMSOF%20(INFLECTIONAL,%20gh2886) (accessed on 15 January 2026).
25. Rinkel, M.W.; von Hoyer, M.E. Groundwater Development in the Area South-West of De Aar. Department of Water, Pretoria. 1976_GH2895. Available online: https://www.dws.gov.za/ghreport/Home/Result.aspx?Search=%20FORMSOF%20(INFLECTIONAL,%20gh2895) (accessed on 28 February 2026).
26. Baloyi, L.; Kanyerere, T.; Muchingami, I.; Pienaar, H.; Igwebuike, N.; Mukhawana, M.B. Utilizing Aquifer Hydraulic Parameters to Assess Local and Regional Recharge Potentials for Enhancing Water Allocations in Groundwater-Dependent Areas in De Aar, Northern Cape, South Africa. *Water* **2025**, *17*, 2709. [CrossRef]
27. Republic of South Africa, Department of Water Affairs. *A Guideline for the Assessment, Planning and Management of Groundwater Resources in South Africa*, 2nd ed.; Republic of South Africa, Department of Water Affairs: Pretoria, South Africa, 2008.
28. Vegter, J.R. Groundwater resources for urban supply—De Aar. A Concise Exposition for Planning Purposes. Dept. Water Pretoria. 1990_GH3710. Available online: https://www.dws.gov.za/ghreport/Home/Result.aspx?Search=%20FORMSOF%20(INFLECTIONAL,%20gh3710) (accessed on 2 March 2026).

29. Strydom, T.; Nel, J.M.; Nel, M.; Petersen, R.M.; Ramjukadh, C.L. The use of radon (Rn222) isotopes to detect groundwater discharge in streams draining table mountain group (tmg) aquifers. *Water SA* **2021**, *47*, 194–199. [CrossRef]
30. Rajmohan, N.; Prathapar, S.A. Assessment of geochemical processes in the unconfined and confined aquifers in the Eastern Ganges Basin: A geochemical approach. *Environ. Earth Sci.* **2016**, *75*, 1212. [CrossRef]
31. Gao, Z.; Tong, H.; Su, Q.; Liu, J.; Gao, F.; Han, C. Hydrochemical characteristics and cause analysis of natural water in the southeast of Qinghai-Tibet Plateau. *Water* **2021**, *13*, 3345. [CrossRef]
32. Ghosh, S.; Jha, M.K. Hydrogeochemical characterization of groundwater and critical assessment of its quality in a coastal basin. *Environ. Dev. Sustain.* **2025**, *27*, 765–830. [CrossRef]
33. Abiye, T.; Verhagen, B.; Freese, C.; Harris, C.; Orchard, C.; Van Wyk, E.; Tredoux, G.; Pickles, J.; Kollongei, J.; Xiao, L. *The Use of Isotope Hydrology to Characterize and Assess Water Resources in South (ern) Africa*; WRC Report No. TT570/13; Water Research Commission (WRC): Pretoria, South Africa, 2013; p. 211.
34. van Wyk, E.; van Tonder, G.; Vermeulen, D. Characteristics of local groundwater recharge cycles in South African semi-arid hard rock terrains: Rainfall-groundwater interaction. *Water SA* **2012**, *38*, 747–754. [CrossRef]
35. Regina, W.E.; Ebia, V.A.; Takang, A.V.; Jude, N.N.; Kimbi, M.B.; Promise, M.G.; Agbor, M.; Boris, M. Stable Isotope Assessment of Groundwater Recharge and Climatic Sensitivity in the N'Kappa Coastal Aquifer, Cameroon. *J. Environ. Geogr. Stud.* **2025**, *4*, 11–33. [CrossRef]
36. Allen, M.; Boutt, D. Environmental Tracers Tritium 3H and SF6 Used to Improve Knowledge of Groundwater Sustainability of a Crystalline Rock Island Aquifer of Tobago, West Indies. *Water* **2023**, *15*, 4231. [CrossRef]
37. Van Rooyen, J.D. Investigating Regional Recharge Dynamics Through the Use of Tritium and Radiocarbon Isotopes to Assess the Hydrological Resilience of Groundwater in Southern Africa. 2021. Available online: https://scholar.sun.ac.za/handle/10019.1/109868 (accessed on 2 March 2026).
38. Schmidt, A.; Schubert, M. Using radon-222 for tracing groundwater discharge into an open-pit lignite mining lake—A case study. In *Isotopes in Environmental and Health Studies*; Taylor & Francis: New York, NY, USA, 2007; pp. 387–400. [CrossRef]
39. Diphofe, K.; Diamond, R.; Kotze, F. Quantifying Baseflow with Radon, H and O Isotopes and Field Parameters in the Urbanized Catchment of the Little Jukskei River, Johannesburg. *Hydrology* **2025**, *12*, 203. [CrossRef]
40. Ali, A.H.; Jassim, A.S.; Abojassim, A.A.; Dosh, R.J. Health Risk Assessment of Radon Concentrations in Water Samples of Selected Areas North of Al-Najaf Governorates. *WSEAS Trans. Environ. Dev.* **2024**, *20*, 895–901. [CrossRef]
41. Eilers, A.; Miller, J.; Swana, K.; Botha, R.; Talma, S.; Newman, R.; Murray, R.; Vengosh, A. Characterisation of Radon Concentrations in Karoo Groundwater, South Africa, as a Prelude to Potential Shale-gas Development. *Procedia Earth Planet. Sci.* **2015**, *13*, 269–272. [CrossRef]
42. Ismail, N.F.; Hashim, S.; Sanusi, M.S.M.; Rahman, A.T.A.; Bradley, D.A. Radon levels of water sources in the southwest coastal region of Peninsular Malaysia. *Appl. Sci.* **2021**, *11*, 6842. [CrossRef]
43. Craig, H. Isotopic Variations in Meteoric Waters. *Science* **1961**, *133*, 1702–1703. [CrossRef]
44. Van Wyk, E. Estimation of Episodic Groundwater Recharge in Semi-Arid Fractured Hard Rock Aquifers. Ph.D. Thesis, University of the Free State, Bloemfontein, South Africa, 2010.
45. Cartwright, I.; Cendón, D.; Currell, M.; Meredith, K. A review of radioactive isotopes and other residence time tracers in understanding groundwater recharge: Possibilities, challenges, and limitations. *J. Hydrol.* **2017**, *555*, 797–811. [CrossRef]
46. Álvarez-Alonso, R.; Ardila, P.R.; Deudero, S.; Melo-Aguilar, C.A.; Alomar, C.; Micheo, F.; Durán, J.J.; Pérez, S.; Cabrera, F.Á.; Pérez, S.M. Multivariate assessment of groundwater contamination levels associated with saline intrusion processes in Mediterranean coastal aquifers. *J. Contam. Hydrol.* **2026**, *278*, 104877. [CrossRef] [PubMed]
47. Adams, S.; Titus, R.; Xu, Y. *Groundwater Recharge Assessment of the Basement Aquifers of Central Namaqualand: Report to the Water Research Commission*; WRC: Lesquin, France, 2004.
48. Monjerezi, M.; Vogt, R.D.; Aagaard, P.; Gebru, A.G.; Saka, J.D.K. Using 87Sr/86Sr, δ18O and δ2H isotopes along with major chemical composition to assess groundwater salinization in lower Shire valley, Malawi. *Appl. Geochem.* **2011**, *26*, 2201–2214. [CrossRef]
49. Lalumbe, L.; Kanyerere, T. Characterisation of Hydro-Geochemical Processes Influencing Groundwater Quality in Rural Areas: A Case Study of Soutpansberg Region, Limpopo Province, South Africa. *Water* **2022**, *14*, 1972. [CrossRef]
50. Madlala, T.; Kanyerere, T.; Oberholster, P.; Butler, M. Assessing the groundwater dependence of valley bottom wetlands in coal-mining environment using multiple environmental tracers, Mpumalanga, South Africa. *Sustain. Water Resour. Manag.* **2021**, *7*, 55. [CrossRef]
51. Yeh, H.-F.; Hsu, K.-C.; Wang, C.-H. Using Stable Isotopes for Assessing the Hydrologic Characteristics and Sources of Groundwater Recharge. *Environ. Eng. Manag. J.* **2009**, *19*, 185–191.
52. Leketa, K.; Abiye, T. Investigating stable isotope effects and moisture trajectories for rainfall events in Johannesburg, South Africa. *Water SA* **2020**, *46*, 429–437. [CrossRef]

53. Tye, A.M.; Milodowski, A.E.; Smedley, P.L. Distribution of Natural Radioactivity in the Environment. 2017. Available online: www.bgs.ac.uk/gsni/ (accessed on 2 March 2026).
54. Casey, N.H.; Meyer, J.A.; Kempster, P.L. *South African Water Quality Guidelines. Vol. 5: Agricultural Use: Livestock Watering*; Department of Water Affairs and Forestry (DWAF): Pretoria, South Africa, 1996.
55. Holmes, S. *South African Water Quality Guidelines. Volume 4. Agricultural Use: Irrigation*; Department of Water Affairs and Forestry: Pretoria, South Africa, 1996; p. 194.